ELSEVIER

Catalysis Today 33 (1997) 25–37

CATALYSIS TODAY

A comparison of steady-state and unsteady-state reaction kinetics of *n*-butane oxidation over VPO catalysts using a TAP-2 reactor system

Yves Schuurman, John T. Gleaves *

Department of Chemical Engineering, Washington University, 1 Brookings Drive, St. Louis, MO 63130, USA

Abstract

The reaction of *n*-butane with 'reactor-equilibrated' $(VO)_2P_2O_7$ based catalysts has been investigated using a combination of low-pressure transient response experiments and atmospheric-pressure steady-flow reaction experiments. The activation energy for *n*-butane conversion in both steady-flow and transient response experiments was a function of the oxidation state of the catalyst. Under steady-flow conditions an activation energy of 17 ± 2 kcal/mol was obtained for 'reactor-equilibrated' catalysts, and 13 ± 2 kcal/mol for an oxygen-treated catalyst. The activation energy for *n*-butane conversion in transient-response experiments varied between 12 ± 1 and 23 ± 2 kcal/mol. An analysis of the transient response curves of the reaction products shows that the rates of formation and desorption of products are strong functions of the catalyst oxidation state. Analysis of the kinetic results indicated that the same sites are involved in the steady-state and unsteady-state conversion of *n*-butane.

Keywords: Steady-state; Unsteady-state; Reaction kinetics; *n*-Butane oxidation; VPO catalysts; TAP-2 reactor system

1. Introduction

The selective oxidation of *n*-butane to maleic anhydride (MA) over vanadium phosphorus oxide (VPO) catalysts has been studied extensively over the past 20 years [1]. Currently, the *n*-butane to MA process is the only industrially practised heterogeneous selective oxidation involving an alkane, and there is strong interest in gaining a fundamental understanding of how the system functions. The selective conversion of alkanes to oxygenates has great practical significance since alkanes are lower-cost feedstocks than their olefin counterparts, and are currently under utilized. A fundamental understanding of how VPO catalysts operate would be an important tool for developing new classes of catalytic materials for alkane oxidation.

A key issue that has not been resolved in *n*-butane oxidation over VPO is the nature of the active-selective phase or phases. Although there is extensive evidence [1–6] that $(VO)_2P_2O_7$ is an essential element in active-selective VPO catalysts, it is not clear how the $(VO)_2P_2O_7$ lattice supplies the 7 oxygen atoms needed to convert *n*-butane to MA. One proposal is that the oxidation primarily involves oxygen adspecies adsorbed at vanadium surface sites, and relatively little bulk lattice oxygen. This idea is supported by a number of studies

* Corresponding author. E-mail: klatu_00@wuche1.wustl.edu.

PII S0920-5861(96)00115-0

[4] measuring the active oxygen on $(VO)_2P_2O_7$ that indicate a close correspondence between the number of surface vanadium atoms, and the amount of active oxygen. However, studies [7,8] of the redox properties of supported VPO catalyst systems, indicate that the amount of active oxygen can exceed the amount of surface oxygen. A number of researchers [9] have proposed that other crystalline phases are involved in the VPO system, and recent TAP-2 reactor studies [10,11] clearly indicate that oxygen adspecies are not the only source of active-selective oxygen.

An important feature of the VPO system is the facile formation and interconversion, at catalytic conditions, of $(VO)_2P_2O_7$, and a number of V^{5+} phases including β-$VOPO_4$, α_{II}-$VOPO_4$, $^{\gamma}$-$VOPO_4$, and δ-$VOPO_4$. There is evidence that $(VO)_2P_2O_7$ samples predominantly exhibiting the (100) face can be topotactically transformed into δ-$VOPO_4$ and back again to the V^{4+} phase at reaction temperatures [12,13]. Recent Raman spectroscopic [9] studies indicate that V^{5+} phases may play an important role in catalyst performance, and suggest that the active sites for maleic anhydride production are situated at the $VOPO_4/(VO)_2P_2O_7$ interface. Other studies comparing the rates of formation and decomposition of maleic anhydride suggest that the formation rate of maleic anhydride depends on the surface distribution of V^{5+} sites, and that the sites must be isolated in order not to yield CO_2 [14,15]. Recent TAP-2 transient response studies [10,11] using 'reactor-equilibrated' $(VO)_2P_2O_7$ catalysts activated with different oxygen treatments indicate that the $(VO)_2P_2O_7$ is readily oxidized at reaction conditions, and that the 'oxygen-treated' catalysts are more active and selective than the 'reactor-equilibrated' catalysts.

Steady-state kinetic studies of *n*-butane oxidation over VPO by a number of groups [15–17] have yielded different steady-state rate expressions and kinetic parameters. For example, literature values for the activation energy of *n*-butane conversion over VPO range from 11 to 27 kcal/mol. In recent vacuum transient-response kinetic studies [11], the activation energy for *n*-butane conversion in the absence of gas phase oxygen was found to be a function of the catalyst surface oxidation state. The activation energy was lower for more highly oxidized samples. It was also reported that the combined rate of MA formation and desorption is faster on the more oxidized surface. The results from the anaerobic transient-response experiments suggest that the differences in steady-state activation energies observed by other workers [15–17] may also be due to differences in catalyst oxidation states. Certain characteristics of industrial fixed-bed *n*-butane processes also suggest that higher surface oxidation states may give improved catalyst performance. For example, a well known feature of VPO fixed-bed processes is that 'equilibrated' catalysts show temporary improvements in performance if the butane feed is terminated for a short period, and the catalyst is held at reaction temperatures in air before the butane feed is restarted. It is also observed that higher selectivity is achieved at lower butane to oxygen feed ratios.

The above results suggest that more than one VPO phase may be involved in the selective conversion of *n*-butane to maleic anhydride. It is clear that under nonsteady-state conditions a 'reactor-equilibrated' catalyst can be made more active and selective, and the activation energy for *n*-butane conversion decreased by oxidizing the VPO surface. The link between kinetic studies at steady-state and nonsteady-state conditions has not been firmly established however, and the catalytic process may change as the reaction conditions change. In light of new nonsteady-state processing approaches to butane oxidation [7,8,18] it is of interest to investigate how kinetic parameters change as the catalyst surface oxidation state changes. The purpose of this paper is to compare kinetic parameters for *n*-butane conversion determined under steady-state conditions at atmospheric pressures with those determined under nonsteady-state conditions at vacuum pressures, and to develop a

reaction model for *n*-butane conversion that is consistent with the experimental data determined in both regimes.

2. Experimental

2.1. Catalyst preparation

Vanadium phosphorus oxide catalysts were prepared by refluxing a mixture of 7340 cm^3 of isobutyl alcohol, 513.5 g of V_2O_5 and 663.97 g of H_3PO_4 (100%) for 16 h to give a light blue precipitate. Upon cooling the precipitate was filtered and dried at ambient temperature under vacuum. The dried precipitate was washed with isobutyl alcohol, dried for 2.5 h at 145°C and calcined in air for 1 h at 400°C. The resulting powder was then charged to a 122 cm long, 2.1 cm i.d. fixed-bed tubular reactor for performance testing. Tests were conducted at a fixed set of reactor conditions of 1.5% butane, 15 psig reactor inlet pressure and 2000 GHSV. After a sufficient break-in period ($\approx$ 500 h) the catalyst gave steady-state selectivities to MA of approximately 66% at 78% conversion. The catalyst samples used in this study were operated at these conditions for approximately 3000 h and were designated 'reactor-equilibrated'. XRD analysis of the reactor-equilibrated samples showed that they were monophasic $(VO)_2P_2O_7$. Chemical analysis gave a P/V ratio of 1.01 and vanadium oxidation state of 4.02. The samples had a BET surface area of 16.5 m^2/g.

2.2. TAP-2 multifunctional reactor system

Steady-state reaction studies, transient response experiments, and oxygen activation experiments were performed with a TAP-2 multifunctional reactor system. A simplified schematic of the TAP-2 system is shown in Fig. 1. The system is comprised of (1) a high-throughput, liquid nitrogen trapped, ultra-high vacuum system, (2) a microreactor-oven assembly with temperature controller, (3) a heatable gas manifold with five input ports containing four pulse valves, and one manual bleed valve, (4) a valve control module for actuating the pulse valves, (5) a gas blending station for preparing reactant mixtures from gases and liquids, (6) a pressure transducer oven, (7) a quadrupole mass spectrometer (QMS), (8) a Pentium-based computer control and data acquisition system, and (9) a slide valve assembly with heated exhaust line (the exhaust line can be attached to a GC or other external analytical device if desired).

Reactant gases can be introduced into the microreactor as steady flows or transient inputs with pulse widths (FWHH) $\approx$ 250 μs. Reaction products are analyzed in real-time using a quadrupole mass spectrometer. Pulses from separate valves can be introduced as sets of pulses of predetermined length or in a pump-probe format alternating between two valves.

For operation at atmospheric pressures the vacuum system is isolated from the microreactor using a slide valve. This configuration is depicted in Fig. 2a. The slide valve contains an adjustable leak valve that controls the amount of reactor effluent that enters the vacuum system. The portion of the effluent that does not escape through the leak valve exits through an external vent that contains an adjustable pressure regulator. When the reactor is operated at atmospheric pressures the mass spectral data can be collected in a standard mass intensity versus mass number format.

When the reactor is operated at vacuum pressures the slide valve is retracted, and the microreactor vents directly into the vacuum system. This configuration is depicted in Fig. 2b. In this case transient response data is collected one mass peak at time in a mass intensity versus time format. The high pumping speed of the vacuum system, and the near proximity of the quadrupole to the microreactor insure that pulses measured by the quadrupole reflect the true microreactor transient response.

All key experimental parameters can be entered from the computer including the reactor

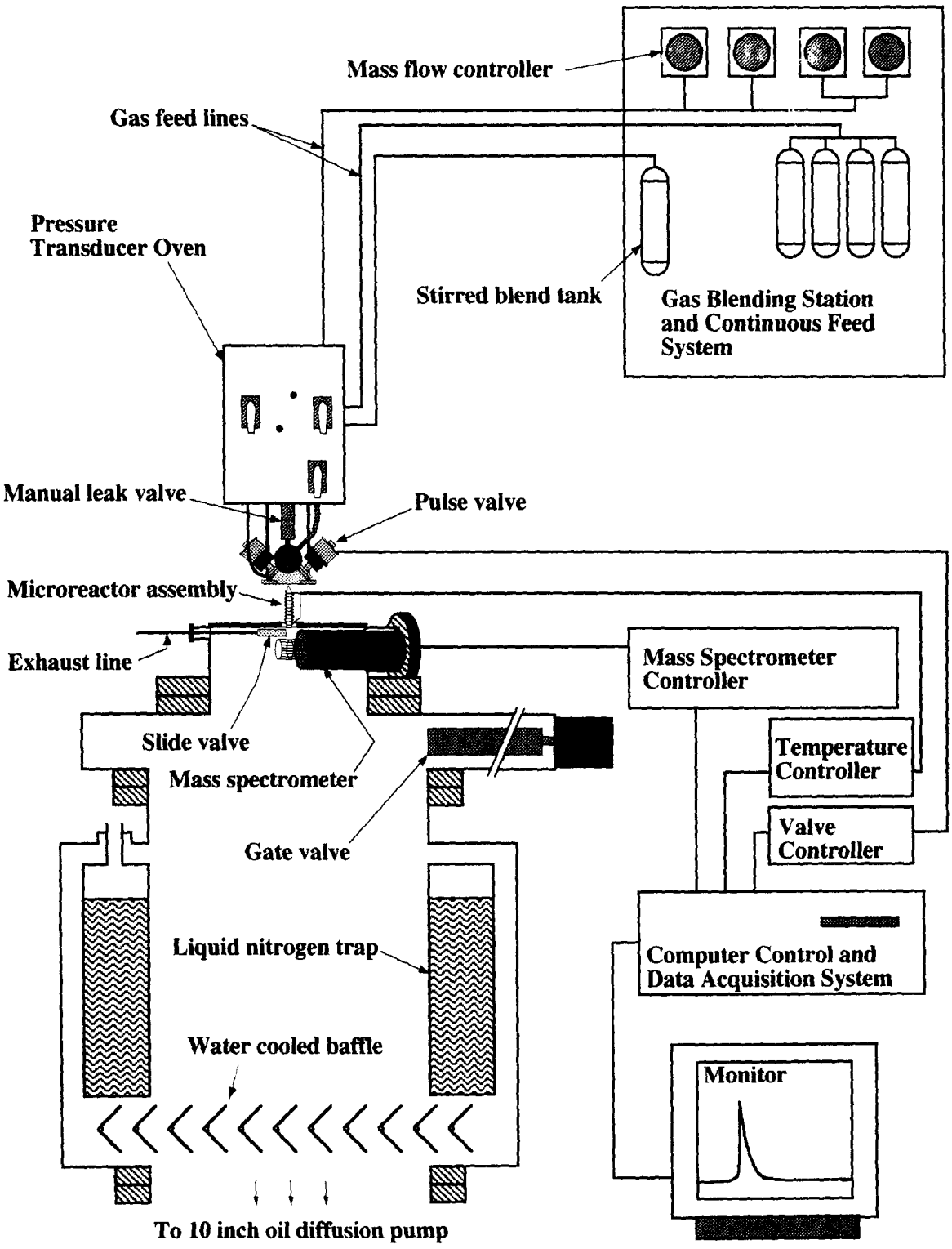

Fig. 1. Simplified schematic of the TAP-2 multifunctional reactor system.

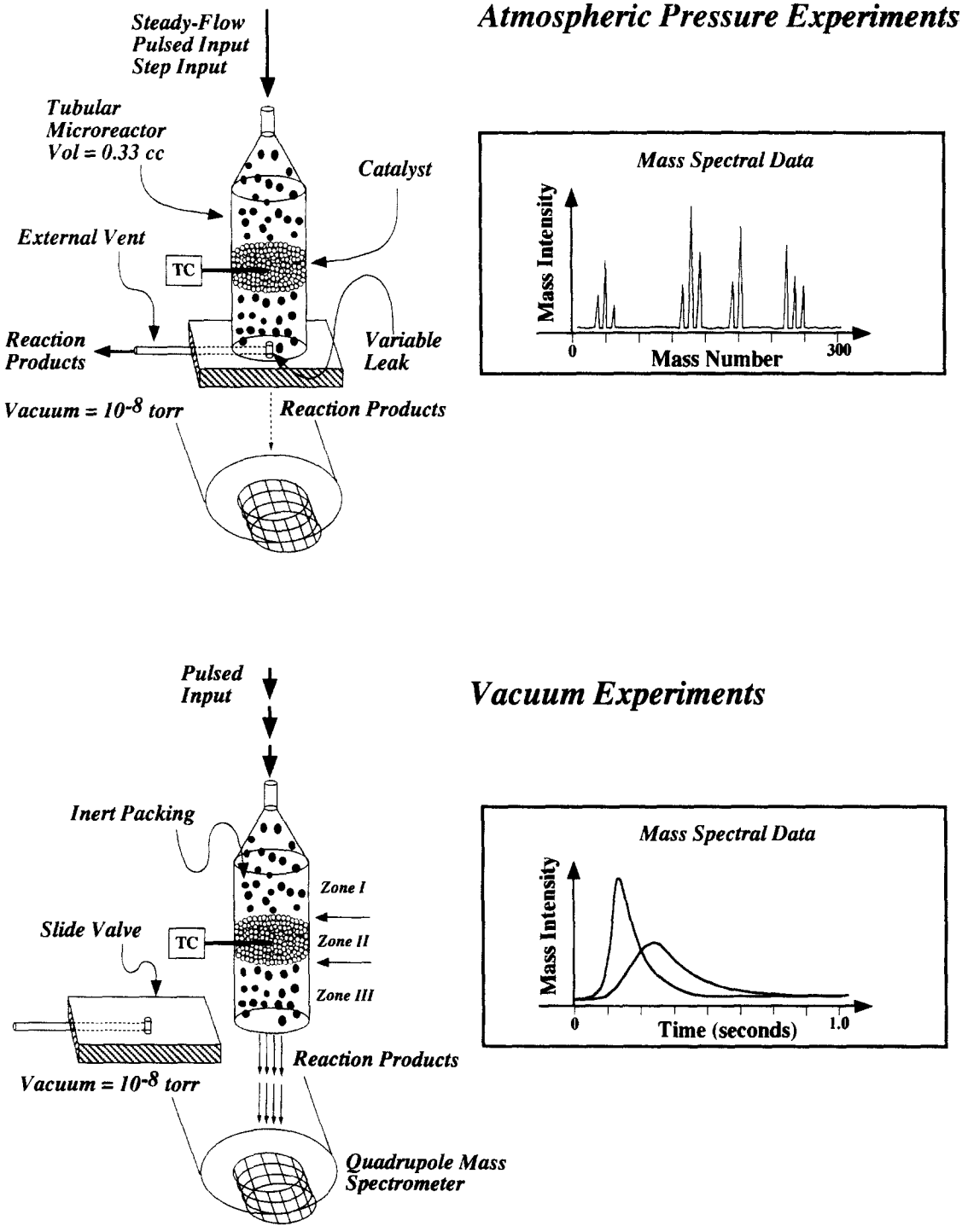

Fig. 2. (a) Microreactor with the slide valve engaged; used for steady-flow experiments at atmospheric pressure. (b) Microreactor continuously evacuated, used for pulse transient experiments.

temperature program, the pulse valve operating sequence, the pulse valve intensity, the data collection time, and the mass spectrometer sensitivity. The data acquisition software has a SCAN mode for collecting conventional mass spectra, and a TRANSIENT mode for collecting high speed transients. The TRANSIENT mode allows sequential collection of up to 5 different mass peaks so that a series of product peaks can be collected in a single experimental run. Both formats can be operated in a temperature programmed mode. Data is stored directly on the computer hard drive during transient experiments, and each product pulse is stored separately. After an experiment is completed the data can be averaged, or each pulse can be viewed individually.

2.3. Procedures

All reaction studies were performed with reactor-equilibrated catalysts samples. A standard charge consisted of 0.1–0.2 g of catalyst with an average particle size of 275 μm. The catalyst bed was centered in the reactor between two zones (designed I and III) of inert glass beads. The inert material is used to thermally insulate the catalyst, and reduce axial temperature gradients in the catalyst bed. Steady-state experiments were performed by flowing a gas blend containing 89% argon, 10% oxygen and 1% *n*-butane at 1.2 atmosphere reactor inlet pressure and flow rates between 0.1 mmol/s and 2 mmol/s. These flow rates ensured turbulent flow, as was shown by a $Re_p > 10$ and by an

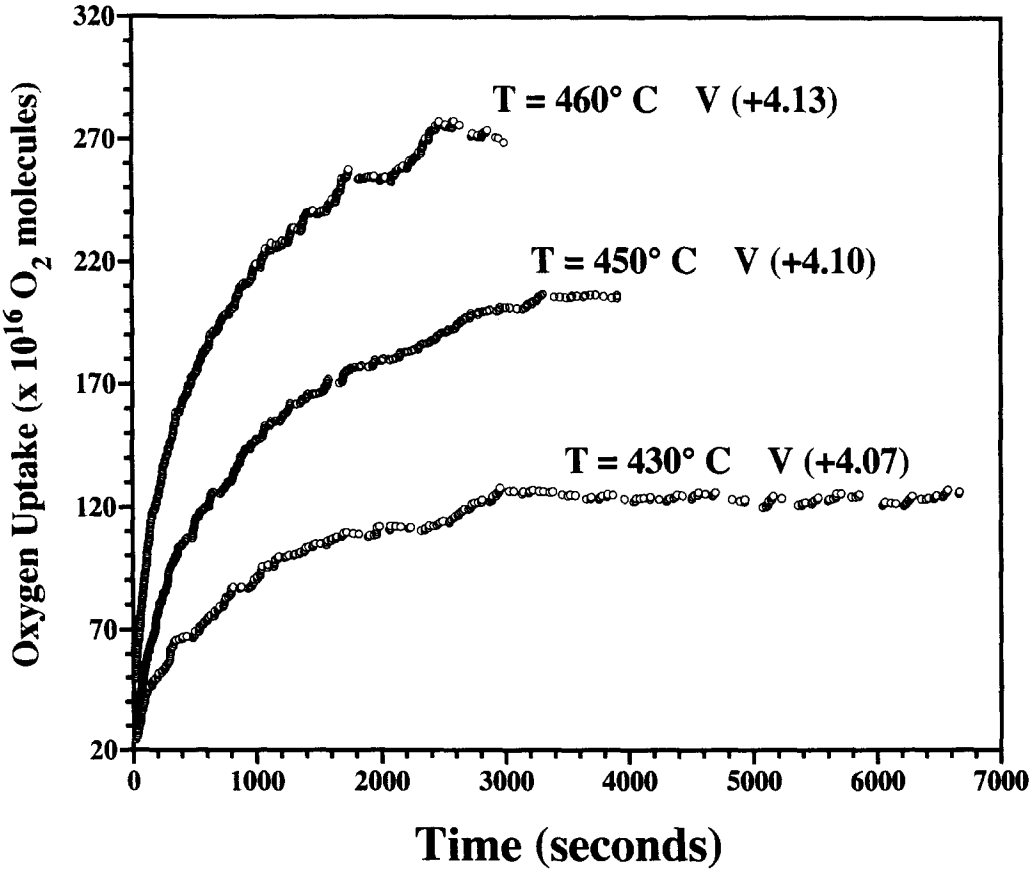

Fig. 3. Oxygen uptake by a 0.1 g sample of 'reactor-equilibrated' VPO at a pressure of 1.2 atm versus time.

analysis of the output response of Xe which was pulsed into the flow at the entrance of the reactor. These conditions together with the fulfilment of $d_t/d_p > 10$ and $L/d_p > 50$ allows the flow through the reactor-bed to be considered as plug flow [19]. Using the maximum reaction rate observed in this study, and the criteria given by Mears [20] it was verified that radial temperature gradients and heat- and mass-transfer limitations were absent. The conversions in steady-state experiments were below 10%, allowing differential data analysis to be used.

Oxygen uptake experiments were performed at constant pressure and constant temperature in the TAP-2 microreactor. Pressure in the microreactor was monitored with a Setra capacitance pressure transducer connected to the external bleed line. The reactor pressure was maintained at a constant value by adding oxygen through one of the pulse valves. The pulse valve firing was computer controlled by continuously monitoring the reactor pressure and pulsing oxygen on an as need basis. The variation in the reactor pressure could be maintained at less than a few torr. The oxygen uptake was determined by determining the number of valve pulses as a function of time.

In a typical oxygen uptake experiment a 'reactor-equilibrated' catalyst charge was first operated at steady-state reaction conditions for 1 h. After 1 h the reactant flow was stopped and the reactor was evacuated. Immediately following evacuation the reactor temperature was adjusted to the temperature of the uptake experiment and a fixed pressure of oxygen was introduced. Fig. 3 shows the oxygen-uptake as a function of time when a reactor equilibrated catalyst is heated at different temperatures and a fixed volume of oxygen with an initial pressure of 1.2 atm is introduced into the microreactor. The oxidation states of the resulting oxygen-treated samples were calculated by assuming that oxygen uptake involves the stoichiometric conversion of $(VO)_2P_2O_7$ to $VOPO_4$.

In addition to the oxygen uptake procedure described above, a continuous flow procedure was used to oxygen-treat catalysts. In this case, the microreactor was operated at a pressure of 1.2 atm, heated to temperatures from 693 to 773 K, and the catalyst was exposed to a continuous flow of pure oxygen for periods ranging from 1 to 60 min. Catalysts oxidized in a continuous flow for 10 min at 723 K behaved the same as catalysts prepared by the analogous oxygen uptake procedure. These catalyst showed the highest activity and selectivity. Catalysts oxidized for longer periods of time were less active, and those completely oxidized (pure oxygen flow at 1.2 atm, 773 K for 60 min) were essentially inactive at reaction temperatures.

Transient response experiments were performed immediately after oxidation treatments or steady-state reaction studies without exposing the catalyst to ambient conditions. In a typical procedure the reactant flow was halted, and the reactor was opened to vacuum. Subsequently, low pressure, isothermal pulse response experiments were carried out at a variety of temperatures (535–698 K). Typical pulse intensities were in the range of 10^{12} to 10^{14} molecules per pulse.

3. Results

Fig. 4 shows the transient responses for argon ($m/e = 40$), *n*-butane ($m/e = 58$), and maleic anhydride ($m/e = 98$) when a 30/1 *n*-butane/argon mixture is pulsed over an oxygen-treated catalyst sample maintained at 698 K. The curves are plotted to show the relative intensities of the parent ions of each species. The absolute pulse intensity was $\approx 10^{12}$ molecules/pulse. Increasing the pulse intensity by an order of magnitude did not change the pulse shape of the inert gas pulse. The independence of the inert gas pulse shape with respect to the pulse intensity indicates that gas transport through the microreactor can be described by Knudsen diffusion [21]. From continuous flow experiments using pure reagents it was deter-

mined that the QMS signals at $m/e = 40$, 58 and 98 were unique to argon, *n*-butane and maleic anhydride, respectively. Therefore the area of the transient responses at these mass numbers is directly proportional to the amount of each species.

After oxidation of the 'reactor-equilibrated' catalyst, a 9/1 mixture of *n*-butane and argon was pulsed over the catalyst at 693 K. Transient response data were collected during this reduction process at different temperatures. Because the transient response experiments were performed at very low pulse intensities (10^{12} molecules/pulse) gas transport can be accurately described as Knudsen diffusion, and the conversion of *n*-butane using a three-zone model represented by the following equations:

$$\text{Zones (I, III)} \quad \epsilon_b \frac{\partial C^j}{\partial t} = D_e^j \frac{\partial^2 C^j}{\partial z^2}, \; j = \text{I, III}$$

$$\text{Zone II (catalyst bed)} \quad \epsilon_b \frac{\partial C^{II}}{\partial t} = D_e^{II} \frac{\partial^2 C^{II}}{\partial z^2} - \epsilon_b k^* C^{II}$$

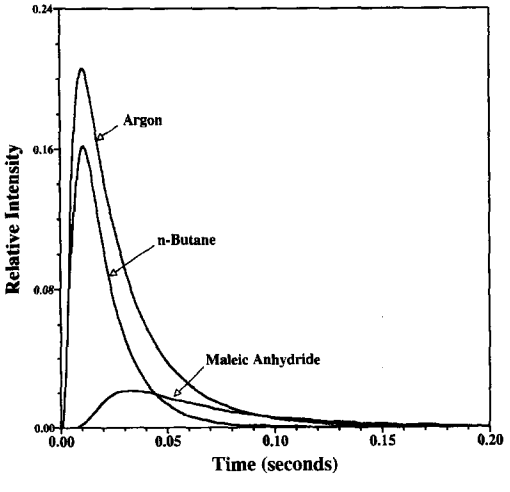

Fig. 4. Transient responses at 698 K of argon ($m/e = 40$), *n*-butane ($m/e = 58$), and maleic anhydride ($m/e = 98$) from a *n*-butane/argon mixture pulsed over an oxygen-treated VPO catalyst sample.

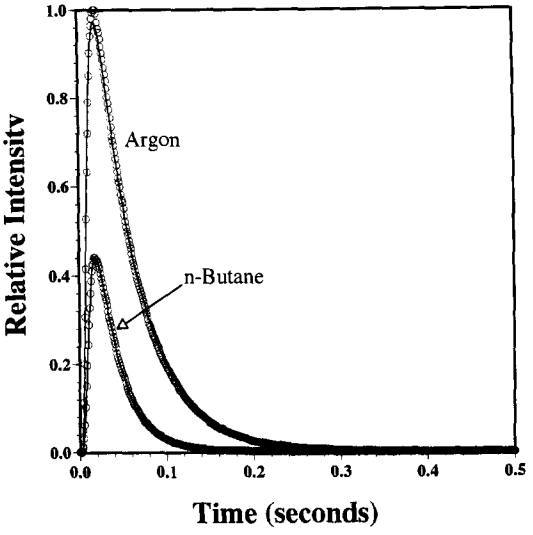

Fig. 5. Experimental (open circles) and model-predicted (solid line) transient responses at 693 K of *n*-butane and argon pulsed over an oxygen-treated VPO catalyst sample.

Boundary and Initial conditions

Zone I	I.C. $t = 0$,	$C^I = 0$
	B.C. $z = 0$, $t > 0$	$-D_e^I \frac{\partial C^I}{\partial z} = \delta(t)$
Zone II	I.C. $t = 0$	$C^{II} = 0$
	B.C. $z = L_I$, $t > 0$	$-D_e^I \frac{\partial C^I}{\partial z} = -D_e^{II} \frac{\partial C^{II}}{\partial z}$
		$C^I = C^{II}$
Zone III	I.C. $t = 0$	$C^{III} = 0$
	B.C. $z = L_{II}$, $t > 0$	$-D_e^{II} \frac{\partial C^{II}}{\partial z} = -D_e^{III} \frac{\partial C^{III}}{\partial z}$
		$C^{II} = C^{III}$
	$z = L$	$C^{III} = 0$

where C = the concentration of *n*-butane, D_e is the effective Knudsen diffusion coefficient, ϵ_b is the bed porosity, k^* is the reaction rate constant multiplied by the number of surface sites (apparent rate constant), and z is the reactor axial coordinate. The number of surface sites is much larger than the number of adsorbing molecules in a pulse, and as result the surface coverage of reactants and products is neglected. It is assumed that *n*-butane chemisorption involves fissure of a CH bond, and that the re-

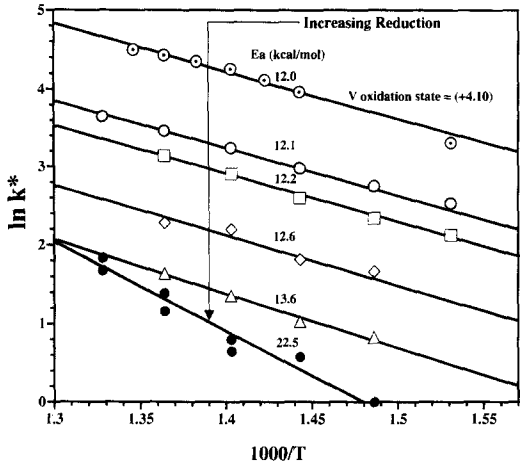

Fig. 6. Arrhenius plots for pulsed *n*-butane conversion over an oxygen-treated VPO catalyst sample. Open circles, experimental data; solid lines, model prediction.

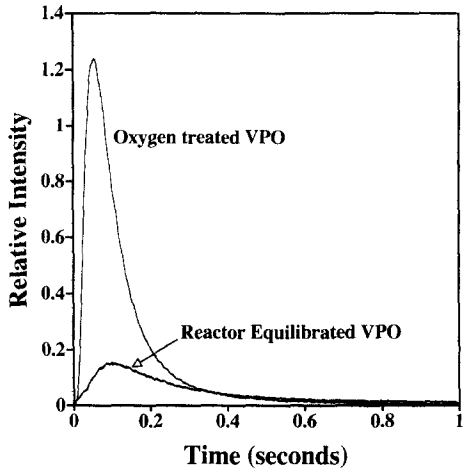

Fig. 7. Transient responses at 673 K of maleic anhydride from a *n*-butane/argon mixture pulsed over an oxygen-treated and 'reactor-equilibrated' VPO catalyst sample.

verse reaction can be neglected. Using the above model and appropriate boundary conditions, the series of *n*–butane transient responses that were obtained during the reduction process were modeled at various temperatures. The curves were modeled using k^* as the only parameter

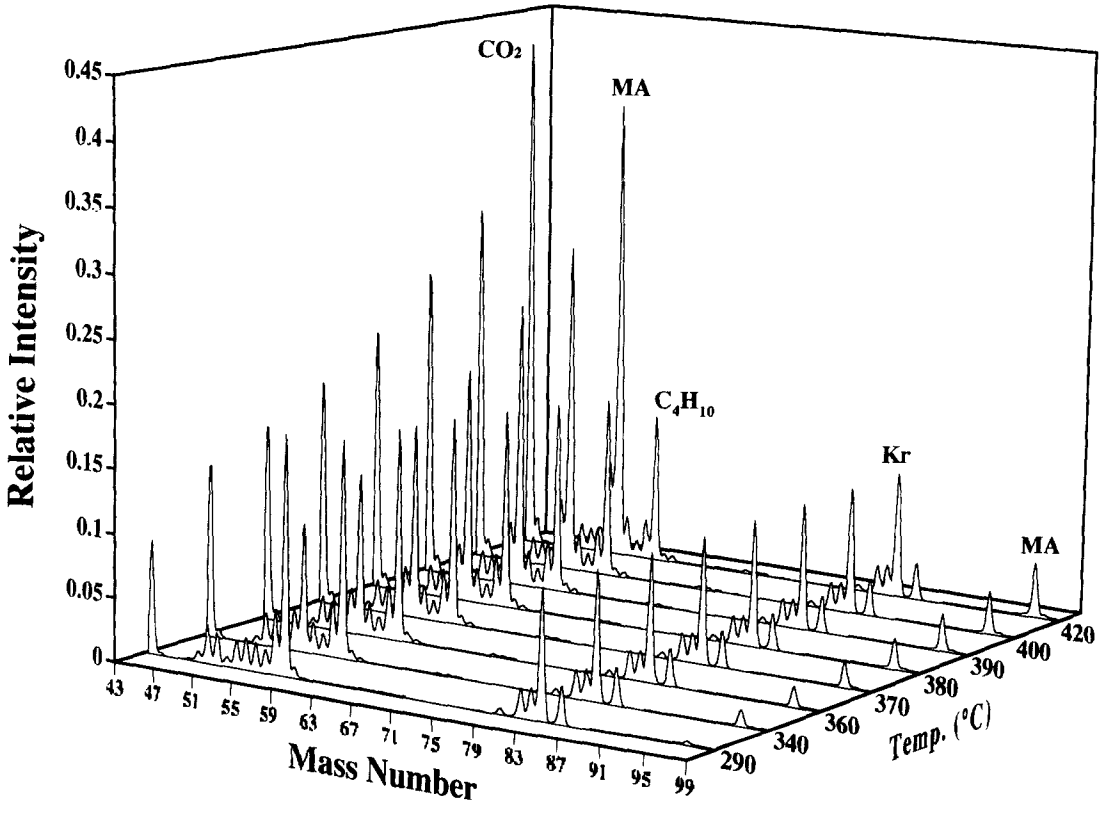

Fig. 8. Mass spectra of steady-flow reaction mixture as a function of temperature when a mixture of *n*-butane, oxygen and krypton is fed over a 'reactor-equilibrated' VPO catalyst.

to be estimated. The diffusivity was obtained by modelling the *n*-butane transient response data at zero conversion, and the porosity was calculated from the mean particle diameter. Typical *n*-butane and argon transient responses and model fits at 693 K are shown in Fig. 5.

The apparent rate constant k^* is plotted versus $1/T$ in the Arrhenius plot shown in Fig. 6. The first transient data taken over the oxidized catalyst show an activation energy of 12.0 kcal/mol. Further pulsing of *n*-butane results in a decrease of the apparent rate constant, and a gradual increase in the activation energy to a final value of 22.5 kcal/mol.

Fig. 7 shows the MA transient responses from pulsing *n*-butane at 673 K over a 'reactor-equilibrated' catalyst sample before and after oxygen treatment. When the pulse areas of the MA responses from the reactor equilibrated and oxygen treated samples were compared, it was found that the response from the more highly oxidized surface is ≈ 4 times larger. In addition, the larger response is more narrow. The difference in the width of the response curves indicates that the combined rate of MA formation and desorption is faster on the more oxidized surface. Previous transient response experiments using MA as an input gas indicate that the largest contribution to the MA pulse width is the slow rate of desorption of MA from the V^{4+} surface. In comparison, when MA is pulsed over a $VOPO_4$ sample the pulse response is relatively narrow indicating MA is weakly adsorbed on a V^{5+} surface.

Fig. 8 shows a series of the mass spectral plots as a function of temperature obtained from a mixture of *n*-butane, oxygen and krypton fed over a reactor equilibrated catalyst. The reaction rate for *n*-butane conversion as function of temperature was calculated from the change in the $m/e = 58$ parent peak. The parent peak of krypton was used as an internal standard. To investigate the effect of the surface oxidation state on the reaction rate under steady-flow conditions a similar series of spectra were obtained after first oxygen-treating the same 'reactor-equilibrated'

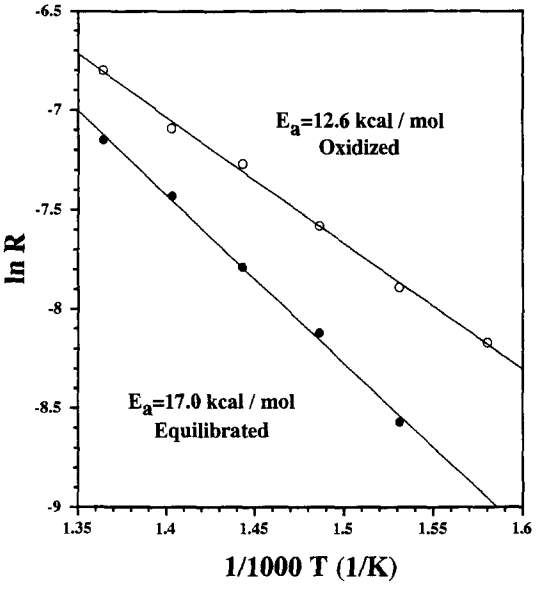

Fig. 9. Arrhenius plots for steady flow *n*-butane conversion over a 'reactor-equilibrated' (full circles) and oxygen-treated (open circles) VPO catalyst sample.

sample in one atmosphere of oxygen for 10 min at 450°C. After an oxygen treatment, the reactor temperature was dropped to the reaction temperature, and the feed was switched to the $Ar/Bu/O_2$ blend. Immediately, after switching the feed a mass spectrum of the reaction was obtained. Within a few minutes after the initial spectrum the *n*-butane conversion would return to the level before the catalyst was oxidized. The oxygen treatment procedure was repeated for each temperature. Arrhenius plots for *n*-butane conversion over a 'reactor-equilibrated' catalyst and an oxygen-treated catalyst is shown in Fig. 9. An apparent activation energy of 17 kcal/mol was obtained for reaction over the 'reactor-equilibrated' catalyst, and 12 kcal/mol for reaction over the oxygen-treated catalyst.

4. Discussion

In recent years there has been considerable debate as to the nature of the active-selective phase in VPO based catalysts. Post-mortem structural studies of 'reactor-equilibrated' cata-

lysts have clearly shown that the predominate crystalline phase in working VPO catalysts is $(VO)_2P_2O_7$ [1–6,9]. It is also well established that $VOPO_4$ compounds by themselves are less selective than $(VO)_2P_2O_7$ [1–6,9]. As a result, many researchers have proposed that $(VO)_2P_2O_7$ is the active-selective phase, although it is generally accepted that V^{5+} species play an important role in the process. Recently published vacuum transient response experiments have shown however, that when the surface of a 'reactor-equilibrated' catalyst is oxidized prior to reaction with *n*-butane the catalysts' selectivity and activity increases significantly. This result strongly suggests that with oxygen-treated catalysts, in the absence of gas phase oxygen, the active-selective site involves a combination of V^{4+} and V^{5+} phases. The results presented in this paper are consistent with this idea, and indicate that the VPO system can be represented by a two site model.

The series of Arrhenius plots displayed in Fig. 6 show that k^* decreases when an oxygen-treated VPO catalyst is reduced by exposure to a series of anaerobic *n*-butane pulses. When the catalyst surface is highly oxidized (the average V oxidation state = 4.10 +) the activation energy for *n*-butane conversion is $\approx$ 12 kcal/mol. After reduction (the average V oxidation state $\approx$ 4.00 +) the activation energy is $\approx$ 23 kcal/mol. The observed decrease in k^* and increase in the activation energy can be accounted for by a two site model with a low activation energy site and a high activation energy site. The low energy site is assumed to be associated with a V^{5+} phase that is formed as the catalyst surface is oxidized, and the high energy site is assumed to be located on the V^{4+} surface. As the catalyst is reduced the V^{5+} concentration and the number of low energy sites decreases. Reduction of the surface simultaneously increases the concentration of high energy sites, and the ratio between the number of high energy sites and the number of low energy sites. The net effect is that the activation energy increases and the reaction rate decreases with reduction of the surface, but a significant increase in the activation energy only occurs when almost all of the low energy sites have disappeared.

The solid lines plotted with the experimental points in Fig. 6 were calculated using the above two site model in which the apparent rate constant k^* is given by

$$k^* = k_1^* \exp(-22.5/RT) + k_2^* \exp(-12.0/RT)$$

where $k_1^* = k_1 N_4$, $k_2^* = k_2 N_5$ and N_4 represents the number of high energy sites on the V^{4+} surface, and the N_5 number of low energy sites associated with the V^{5+} phase. The model curves for reaction on a surface containing both V^{4+} and V^{5+} phases were obtained by simultaneously varying the magnitudes of k_1^* and k_2^*. It was assumed that changes in k_1^* and k_2^* result from a change in the relative number of V^{4+} and V^{5+} sites, and that the per site preexponential factors k_1 and k_2 do not depend on the overall oxidation state of the catalyst.

Assuming each high energy site is associated with one surface vanadium atom, the upper limit to the total number of high energy sites can be estimated at 1×10^{23} sites/kg cat. The observable preexponential factor for reaction on the V^{4+} surface can be calculated from the above expression for k^* by assuming that the lowest Arrhenius plot is for reaction on the V^{4+} surface alone. With this assumption a value for k_1^* of 2×10^7 s^{-1} is obtained. Assuming a value of 1×10^{23} sites/kg cat for the number of high energy sites then the preexponential factor per site, k_1, is 2×10^{-16} kg cat/site s. If the assumed number of high energy sites is made lower, then k_1 must be increased since the product $k_1 N_4$ is fixed.

Assuming each high energy site is converted to a low energy site during the oxygen treatment process the number of low energy sites on the most active oxygen treated catalyst can be estimated at 1×10^{23} sites/kg cat, and the value of k_2 at 3×10^{-18} kg cat/site s. A two orders of magnitude decrease in the preexponential factor could result from a change in the structure of

the active site. On the other hand, if k_2 is approximately equal to k_1, then the number of low energy sites generated during the oxidation treatment must be much less than number of high energy sites.

Chemical analysis and oxygen uptake curves of the oxygen-treated catalyst indicate that 10% of the total vanadium is in the V^{5+} state. Previous oxygen-18 exchange experiments and TPD experiments indicate that when 'reactor-equilibrated' $(VO)_2P_2O_7$ is oxidized the oxygen-18 is incorporated in the surface layers as part of a $VOPO_4$ phase, and on the time scale of our experiments does not diffuse into the bulk. Consequently, it is reasonable to assume that a significant portion of the surface of an oxidized VPO catalyst is composed of $VOPO_4$ phases. Some V^{4+} sites must be present at the surface however, since a completely oxidized surface is inactive. If the number of low energy sites on the most active oxygen treated surface is only a small fraction of the total number of sites, and V^{4+} must be present to have an active surface then the low energy sites are likely to be located at the V^{4+}/V^{5+} phase boundary.

The role of V^{5+} phases in steady-state reactions is less clear. Under steady-state reaction conditions the oxidation state of the VPO catalyst surface is influenced by the composition of the gas phase reaction mixture and the reaction temperature. In general, the surface vanadium oxidation state increases with oxygen partial pressure. As indicated by the oxygen uptake curves presented in Fig. 3 the oxidation rate for a 'reactor-equilibrated' catalyst increases with temperature when the catalyst is heated in an atmosphere of oxygen. Conversely, if an oxygen-treated VPO catalyst is heated in vacuum the catalyst will evolve oxygen and will revert to $(VO)_2P_2O_7$. Chemical analyses of the 'reactor-equilibrated' catalysts used in this study show that $\approx 2.0\%$ of the vanadium is in the V^{5+} oxidation state. As indicated in Fig. 8 the apparent activation energy for *n*-butane oxidation over a 'reactor-equilibrated' catalyst was determined to be 17 kcal/mol. This is in the range of values determined by other researchers [15–17]. However, this value is lower than the activation energy for reaction on a surface with only high energy sites, and indicates the 'reactor-equilibrated' surface contains some low energy sites. The upper Arrhenius plot in Fig. 9 which yields an activation energy of 12.6 kcal/mol indicates the number of low energy sites can be increased temporarily under steady-flow conditions by oxidizing the surface prior to introducing the reaction mixture. The values for the activation energy under steady-flow conditions at atmospheric pressures, and pulsed-flow at vacuum pressures for an oxidized catalyst are very similar indicating the same low energy sites are involved in the reaction mechanism. Using the estimated number of sites determined in the vacuum pulse experiments, and the reaction rates obtained from the steady-flow experiments, a lower limit for the turnover frequency of 1/s for the steady-flow reaction was calculated.

Acknowledgements

The financial support provided by the National Science Foundation grant number CTS-9322829, and Huntsman Chemical Company is gratefully acknowledged. The authors would also like to acknowledge Professor Gregory Yablonskii, Dr. Shaorong Chen, David Dowell, and Pungphai Phanawadee for many fruitful discussions.

References

[1] G. Centi, F. Trifiro, J.R. Ebner and V.M. Franchetti, Chem. Rev., 88 (1988) 55.
[2] G. Stefani, F. Budi, C. Fumagalli and G.D. Suciu, Chim. Ind. (Milan), 72 (1990) 604.
[3] G. Stefani, F. Budi, C. Fumagalli and G.D. Suciu, in G. Centi and F. Trifiro, Editors, New Developments in Selective Oxidation, Elsevier, Amsterdam, 1990, p. 537.
[4] J.R. Ebner and J.T. Gleaves, in A.E. Martell and D.T. Sawyer, Editors, Oxygen Complexes and Oxygen Activation by Transition Metals, Plenum, 1988, p. 273.

[5] G. Cent, F. Trifiro, G. Busca, J.R.Ebner and J.T. Gleaves, Faraday Discuss. Chem. Soc., 87 (1989) 215.
[6] G. Centi, Catal. Today, 16 (1993) 5, and references therein.
[7] R.M. Contractor, H.E. Bergna, H.S. Horowitz, C.M. Blackstone, U. Chowdhry and A.W. Sleight, Catalysis, 38 (1987) 645.
[8] R. Contractor, J.R. Ebner and M.J. Mummey, New Dev. Select. Oxidat., 55 (1990) 553.
[9] Y. Zhang, R.P.A. Sneeden and J.C. Volta, Catal. Today, 16 (1993) 39.
[10] Y. Schuurman, J.T. Gleaves, J.R. Ebner and M.J. Mummey, in V. Cortes Corberan and S.V. Bellon, Editors, New Developments in Selective Oxidation II, Elsevier, Amsterdam, 1994.
[11] Y. Schuurman and J.T. Gleaves, Ind. and Eng. Chem. Res., 33 (1994) 2935.
[12] E. Bordes, Catal. Today, 16 (1993) 27.
[13] T.P. Moser and G.L. Schrader, J. Catal., 104 (1987) 99.
[14] M.E. Lashier and G.L. Schrader, J. Catal. 128 (1991) 113.
[15] S.K. Bej and M.S. Rao, Ind. Eng. Chem. Res. 30 (1991) 1819.
[16] J.S. Buchanan and S. Sundaresan, Appl. Catal., 26 (1986) 211.
[17] P. Schnider, G. Emig and H. Hofmann, Ind. Eng. Chem. Res., 26 (1987) 2236.
[18] J.J. Lerou and P.L. Mills, in Precision Process Technology, Kluwer Academic, Amsterdam, 1993, pp. 175–195.
[19] D.E. Mears, Chem. Eng. Sci., 26 (1971) 1361.
[20] D.E. Mears, J. Catal., 20 (1971) 127.
[21] G.D. Svoboda, J.T. Gleaves and P.L. Mills, Ind. Eng. Chem. Res., 31 (1992) 19.